


***Physaria fendleri* and *Ricinus communis* lecithin:cholesterol acyltransferase-like phospholipases selectively cleave hydroxy acyl chains from phosphatidylcholine**

Yang Xu^{1,†}, Kristian Mark P. Caldo^{1,*}, Stacy D. Singer^{1,2}, Elzbieta Mietkiewska¹, Michael S. Greer¹, Bo Tian^{1,3}, John M. Dyer⁴, Mark Smith⁵, Xue-Rong Zhou⁶, Xiao Qiu⁷, Randall J. Weselake¹ and Guanqun Chen¹ 

¹Department of Agricultural, Food and Nutritional Science, 410 Agriculture/Forestry Centre, University of Alberta, Edmonton, Alberta T6G 2P5, Canada,

²Agriculture and Agri-Food Canada, Lethbridge Research and Development Centre, Lethbridge, Alberta T1J 4B1, Canada,

³CAS Key Laboratory of Tropical Plant Resource and Sustainable Use, Xishuangbanna Tropical Botanical Garden, Chinese Academy of Sciences, Kunming 650223, China,

⁴U.S. Department of Agriculture–Agricultural Research Service, US Arid-Land Agricultural Research Center, Maricopa, AZ 85138, USA,

⁵Agriculture and Agri-Food Canada, 107 Science Place, Saskatoon, Saskatchewan S7N 0X2, Canada,

⁶CSIRO Agriculture and Food, PO Box 1700, Canberra, ACT 2601, Australia,

⁷Department of Food and Bioproduct Sciences, University of Saskatchewan, Saskatoon, Saskatchewan S7N 5A8, Canada

Received 10 July 2020; revised 12 October 2020; accepted 21 October 2020; published online 27 October 2020.

*For correspondence (e-mail gc24@ualberta.ca).

[†]Present address: MSU-DOE Plant Research Laboratory, Michigan State University, East Lansing, MI 48824, USA

[‡]Present address: Department of Biological Sciences, University of Calgary, Calgary, Alberta, T2N 1N4, Canada

SUMMARY

Production of hydroxy fatty acids (HFAs) in transgenic crops represents a promising strategy to meet our demands for specialized plant oils with industrial applications. The expression of *Ricinus communis* (castor) *OLEATE 12-HYDROXYLASE* (*RcFAH12*) in *Arabidopsis* has resulted in only limited accumulation of HFAs in seeds, which probably results from inefficient transfer of HFAs from their site of synthesis (phosphatidylcholine; PC) to triacylglycerol (TAG), especially at the *sn*-1/3 positions of TAG. Phospholipase As (PLAs) may be directly involved in the liberation of HFAs from PC, but the functions of their over-expression in HFA accumulation and distribution at TAG in transgenic plants have not been well studied. In this work, the functions of lecithin:cholesterol acyltransferase-like PLAs (LCAT-PLAs) in HFA biosynthesis were characterized. The LCAT-PLAs were shown to exhibit homology to LCAT and mammalian lysosomal PLA₂, and to contain a conserved and functional Ser/His/Asp catalytic triad. *In vitro* assays revealed that LCAT-PLAs from the HFA-accumulating plant species *Physaria fendleri* (PfLCAT-PLA) and castor (RcLCAT-PLA) could cleave acyl chains at both the *sn*-1 and *sn*-2 positions of PC, and displayed substrate selectivity towards *sn*-2-ricinoleoyl-PC over *sn*-2-oleoyl-PC. Furthermore, co-expression of *RcFAH12* with PfLCAT-PLA or RcLCAT-PLA, but not *Arabidopsis AtLCAT-PLA*, resulted in increased occupation of HFA at the *sn*-1/3 positions of TAG as well as small but insignificant increases in HFA levels in *Arabidopsis* seeds compared with *RcFAH12* expression alone. Therefore, PfLCAT-PLA and RcLCAT-PLA may contribute to HFA turnover on PC, and represent potential candidates for engineering the production of unusual fatty acids in crops.

Keywords: phospholipase A, lecithin:cholesterol acyltransferase-like PLA, hydroxy fatty acid, phosphatidylcholine, triacylglycerol, *Physaria fendleri*, *Ricinus communis*, *Arabidopsis thaliana*.

INTRODUCTION

Hydroxy fatty acids (HFAs; for a full list of the abbreviations used in this study see Appendix S1 in the online Supporting Information) are among the most valuable unusual fatty acids for industrial applications (Ogunniyi, 2006; Bates and

Browse, 2011; Bates *et al.*, 2014; McKeon, 2016; Mubofu, 2016). Hydroxy fatty acids are naturally present in the seeds of a small number of plant species, including castor (*Ricinus communis*), *Hiptage benghalensis* and *Physaria fendleri* (synonym *Lesquerella fendleri*; *Physaria* hereafter), which

contain up to 90% and 70% ricinoleic acid (12-hydroxyoctadec-*cis*-9-enoic acid, 12-OH 18:1 Δ^{9cis}) and 60% lesquerolic acid (14-hydroxyeicos-*cis*-11-enoic acid, 14-OH 20:1 Δ^{11cis}) in their seed oil, respectively (Badami and Kudari, 1970; Chen, 2016; McKeon, 2016; Tian *et al.*, 2019). Ricinoleic acid is synthesized through the hydroxylation of oleic acid (18:1 Δ^{9cis}) on the *sn*-2 position of phosphatidylcholine (PC) via the catalytic action of fatty acid hydroxylase (Bafar *et al.*, 1991; van de Loo *et al.*, 1995). This fatty acid can then undergo further elongation to yield lesquerolic acid in the form of acyl-CoA (Moon *et al.*, 2001).

Despite the fact that PC is the site of HFA biosynthesis, these fatty acids accumulate at high levels in storage triacylglycerol (TAG) but are excluded from membrane lipids in plants that naturally accumulate them (Millar *et al.*, 2000). This suggests that in addition to the traditional Kennedy pathway (Kennedy, 1961), HFA turnover on PC and the subsequent incorporation into TAG must operate efficiently in these plants [for reviews see Bates and Browse (2012) and Bates (2016)]. Turnover of PC was described by Lands (1960), whereby the deacylation of PC and re-acylation of lysophosphatidylcholine (LPC) were suggested to occur through the activities of phospholipase A (PLA) and lysophosphatidylcholine acyltransferase (LPCAT), respectively. The mechanism driving acyl editing, however, is now understood to be far more complex, as an increasing number of enzymes have been found to play a role (Chapman and Ohlrogge, 2012; Bates, 2016).

The PLAs comprise a complex group of enzymes that catalyze the hydrolysis of phospholipids to liberate unesterified fatty acids and have many important physiological roles in a broad spectrum of plant biological processes (Wang, 2001; Munnik and Testerink, 2009; Canonne *et al.*, 2011; Kim *et al.*, 2011; Chen *et al.*, 2011; Li *et al.*, 2013, 2015). In plant seeds that accumulate unusual fatty acids such as HFAs, PLAs have also been reported to play a role in releasing unusual fatty acyl groups from phospholipids (Bayon *et al.*, 2015; Lin *et al.*, 2019). Three families of PLAs have been identified in plants thus far based on the ester bond position of the phospholipids that they act upon. The families include PLA₁, low molecular weight secretory PLA₂ (sPLA₂) and patatin-like PLA (pPLA). PLA₁ and sPLA₂ catalyze the hydrolysis of phospholipids at the *sn*-1 and *sn*-2 positions, respectively, while pPLA acts catalytically at both positions [for a review see Wang (2001)].

Initial attempts to engineer plants to produce HFAs in their seed oil involved the seed-specific over-expression of *OLEATE 12-HYDROXYLASE* from the HFA-accumulating castor plant (*RcFAH12*) in a non-HFA-accumulating plant (such as *Arabidopsis thaliana* or *Camelina sativa*). Limited success was achieved using this approach, with HFAs accumulating to levels up to only approximately 17% of the total seed fatty acids in transgenic lines (Broun and Somerville, 1997; Smith *et al.*, 2003; Lu *et al.*, 2006; Lu and

Kang, 2008). This low level of accumulation was attributed to inefficient transfer of HFA from PC to TAG in the transgenic plants, which further resulted in the feedback inhibition of fatty acid biosynthesis (Bates and Browse, 2011; Bates *et al.*, 2014; Lunn *et al.*, 2019). To liberate HFA from PC, certain castor PLAs acting on the *sn*-2 position of PC, including sPLA₂ α (Bayon *et al.*, 2015) and pPLAIII (Lin *et al.*, 2019), have been co-expressed with *RcFAH12* in the *Arabidopsis fatty acid elongase1 (fae1)* mutant background (Kunst *et al.*, 1992; Lu *et al.*, 2006). The resulting transgenic lines, however, exhibited dramatic decreases in seed HFA content in both PC and TAG when compared with *Arabidopsis* expressing *RcFAH12* alone (Bayon *et al.*, 2015; Lin *et al.*, 2019).

Previously, a lecithin:cholesterol acyltransferase-like PLA was identified in *Arabidopsis* (AtLCAT-PLA) that does not fall neatly into any of the current PLA clades. While this enzyme is closely related to the *Arabidopsis* LCAT-PLA₁ enzyme (Noiriel *et al.*, 2004), it displays both PLA₁ and PLA₂ activities with a preference for hydrolyzing acyl groups at the *sn*-2 position of PC (Chen *et al.*, 2012). Since the physiological functions of LCAT-PLA in plants have yet to be explored, the aim of the current study was to examine its possible contribution to the transfer of unusual fatty acids from PC to TAG. The LCAT-PLAs from *Physaria* (PfLCAT-PLA) or *castor* (RcLCAT-PLA) showed substrate selectivity towards *sn*-1-palmitoyl-*sn*-2-ricinoleoyl-PC (Ric-PC) over *sn*-1-palmitoyl-*sn*-2-oleoyl-PC (18:1-PC) when heterologously produced in yeast. When the coding regions of LCAT-PLAs from different species (*Physaria*, *castor* and *Arabidopsis*) were over-expressed in the *Arabidopsis RcFAH12/fae1* line, respectively, no significant alteration in HFA levels was observed in transgenic *Arabidopsis* seeds compared with *RcFAH12/fae1* lines, which contrasts with the dramatic decreases observed with the expression of sPLA₂ α (Bayon *et al.*, 2015) or pPLAIII (Lin *et al.*, 2019). Further lipid class analysis revealed that the expression of PfLCAT-PLA or RcLCAT-PLA, but not AtLCAT-PLA in a *RcFAH12/fae1* background, enhanced the distribution of HFA at the *sn*-1/3 positions of TAG. Taken together, these results suggest that PfLCAT-PLA and RcLCAT-PLA may contribute to HFA turnover on PC by preferentially cleaving *sn*-2-ricinoleoyl chains, and thus have potential for manipulating production of unusual fatty acids in transgenic plants.

RESULTS

Plant LCAT-PLAs are homologs of LCAT and mammalian lysosomal PLA₂

Considering the catalytic features of AtLCAT-PLA (Chen *et al.*, 2012), it was of interest to identify LCAT-PLAs from *P. fendleri* (PfLCAT-PLA) and *R. communis* (RcLCAT-PLA) and elucidate their possible roles in turnover of PC. Putative PfLCAT-PLA and RcLCAT-PLA homologs were isolated

from *P. fendleri* and *R. communis* cDNAs and shown to share 69.8% pairwise identity with each other, as well as 91% and 68.9% pairwise identities to AtLCAT-PLA, respectively, at the amino acid level. To explore the evolutionary relationship of plant LCAT-PLAs with other PLA and LCAT family members, phylogenetic analysis was carried out using sequences from various species. Plant PLAs were shown to separate into five distinct subgroups, including PLA₁, phosphatidic acid-preferring PLA₁ (PA-PLA₁), sPLA₂, pPLA and LCAT-PLA₁/LCAT-PLA (Figure 1). Plant LCAT-PLAs are grouped with LCAT-PLA₁ enzymes, which are closely related to LCAT and mammalian lysosomal PLA₂ (LPLA₂) and show homology to plant and yeast phospholipid: diacylglycerol acyltransferase (PDAT) and plant phospholipid: sterol *O*-acyltransferase (PSAT).

With the exception of sPLA₂ enzymes, all PLAs possess a highly conserved lipase motif. This motif consists of GX₁SG in all PLA₁, PA-PLA₁ and pPLAI and II proteins, and

XHSXG ([P/S/T/C/A/G]HS[M/L]G; Falarz *et al.*, 2020) in plant LCAT-PLAs and their close orthologs in the LCAT family (Figure 1). More specifically, in plant LCAT-PLA, the first Gly in the lipase motif is substituted with a Ser or Thr, with the exception of LCAT-PLA from *Columba livia* (CILCAT-PLA), which contains the original lipase motif (Figure 1). Similarly, plant PDAT, LCAT, PSAT and mammalian LPLA₂ have a Pro, Ser or Ala in that position, whereas animal LCAT and yeast PDAT have the original Gly. The lipase motif contains the catalytic Ser of the active site, which is a part of the catalytic triad/dyad. The Ser/Asp/His catalytic triad is well conserved among PLA₁, LCAT-PLA and other LCAT-like proteins (LCAT-PLA₁, LCAT, LPLA₂, PDAT, PDST). In contrast, Ser/Asp serves as an essential catalytic dyad for lipid hydrolytic activity in pPLAI, pPLAII and yeast phospholipase B (PLB) enzymes, whereas His/Asp acts as the catalytic dyad in sPLA₂ enzymes. Regarding pPLAIII, it contains a distinctive non-canonical lipase GXG₁XG motif

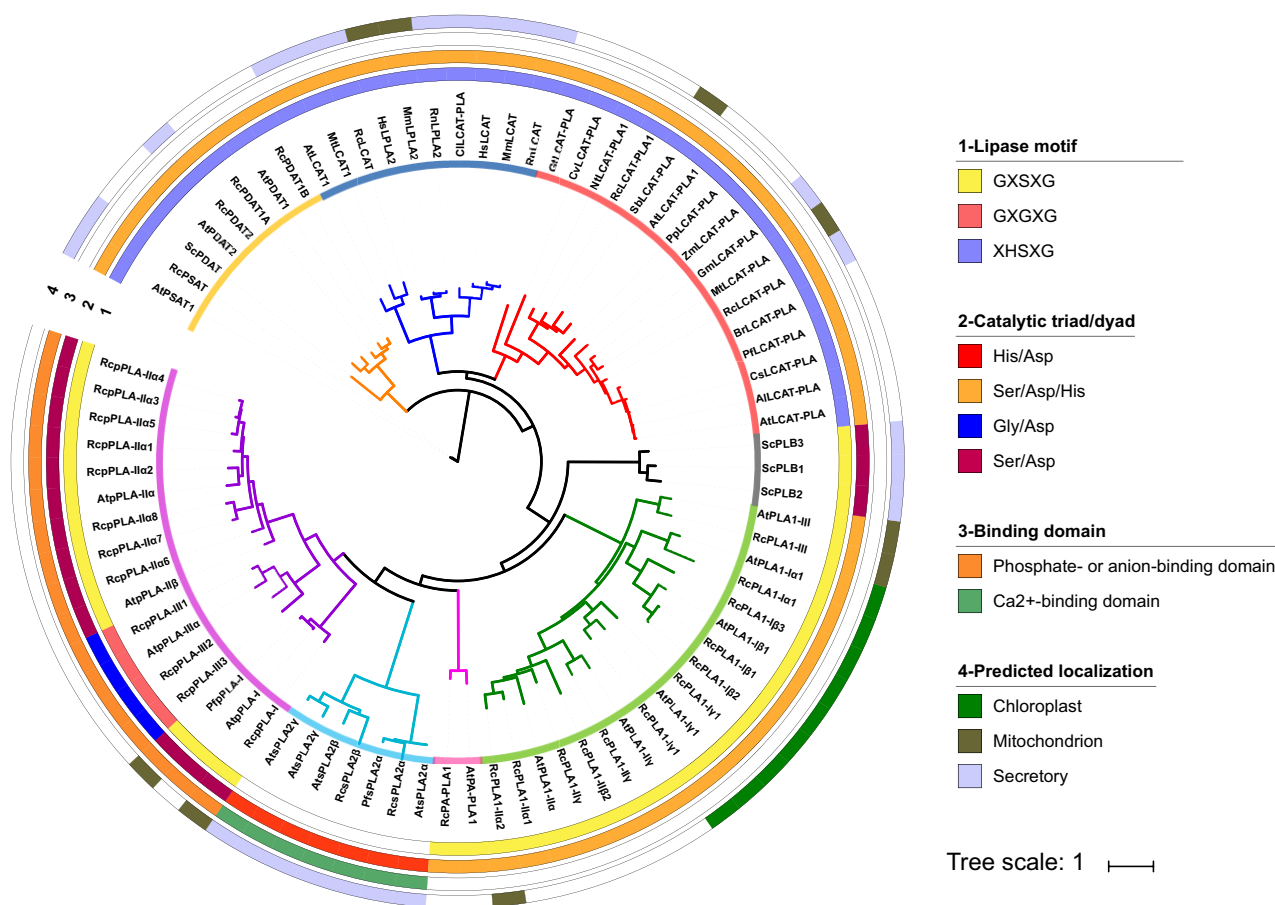


Figure 1. Phylogenetic relationship of lecithin:cholesterol acyltransferase-like phospholipase A (LCAT-PLA), lecithin:cholesterol acyltransferase (LCAT), PLA and other related enzymes from plants and other species.

The maximum likelihood phylogenetic tree was constructed with IQ-TREE. Clades of PLA₁, phosphatidic acid-preferring PLA₁ (PA-PLA₁), secretory PLA₂ (sPLA₂), patatin-like PLA (pPLA), LCAT-PLA, LCAT and lysosomal PLA₂ (LPLA₂), phospholipid: diacylglycerol acyltransferase (PDAT) and phospholipase B (PLB) are shown in green, pink, light blue, purple, red, dark blue, orange and black, respectively. Results of lipase motif, catalytic triad/dyad, and binding domain analyses and the predicted localization of each protein are shown in circle layers 1, 2, 3 and 4, respectively.

instead of GX SXG and a conserved Gly/Asp catalytic dyad. In addition, sPLA₂ and pPLA enzymes also possess a Ca²⁺-binding motif and phosphate- or anion-binding motif, respectively.

The Ser/His/Asp catalytic triad is essential for plant LCAT-PLA enzymatic activity

To gain insight into the function of the conserved Ser/His/Asp catalytic triad in plant LCAT-PLAs (Figure 2a–c), the structure of PflCAT-PLA was predicted using SWISS-MODEL software and *Homo sapiens* LPLA₂ (RCSB 4x92.1) as a template (Glukhova *et al.*, 2015). The three-dimensional model included amino acid residues 30–435, which exhibits 23.01% amino acid identity with the template and contains the catalytic triad residues Ser182, Asp391 and His416. The values of GMQE and QMEAN for the structure were 0.44 and –3.64, respectively, indicating that the model is of good quality. The predicted PflCAT-PLA model structure exhibits an α/β -hydrolase fold with a canonical Ser/His/Asp catalytic triad (Rauwerdink and Kazlauskas, 2015) and active site residues localized within loop regions in the middle of the structure (Figure 2e, boxed). As expected, the catalytic triad residues form polar interactions with one another. The hydroxy group of Ser182 appears to form a hydrogen bond with His416, which in turn forms a polar interaction with Asp391 (Figure 2f).

Site-directed mutagenesis of PflCAT-PLA was utilized to verify the importance of these residues in catalysis. As shown in Figure 2(d), PflCAT-PLA encodes an active enzyme whereas mutation of Ser182, Asp391 or His416 led to dramatic decreases in enzyme activity. The serine within this catalytic triad is typically responsible for attacking the carboxyl carbon in deacylation reactions during hydrolysis. The abolition of PflCAT-PLA activity through the conversion of Ser182 to Ala confirmed its catalytic importance as the nucleophile (Figure 2d,g). Similarly, the substitution of His416 with Ala also drastically affected activity, as this presumably resulted in a loss of the base which activates the serine nucleophile (Figure 2h). In contrast, the loss of Asp391 only led to a partial loss of enzyme activity (Figure 2d). This suggests that, in this mutant, Ser182 interacts with His416 but the loss of Asp391 may reduce the ability of histidine to interact with the serine hydroxy hydrogen, resulting in a less active enzyme (Figure 2i).

This catalytic feature appears to be well conserved among LCAT-PLAs from plants and animals (Figure S1). Structural alignment of PflCAT-PLA with homologous enzymes from *Arabidopsis* (AtLCAT-PLA), *R. communis* (RcLCAT-PLA), *Physcomitrella patens* (PpLCAT-PLA) and *Mus musculus* (MmLCAT-PLA) yielded RMSD values of 0.066, 0.173, 0.370 and 2.642, respectively, indicating that the PflCAT-PLA structure was the most and least similar to AtLCAT-PLA and MmLCAT-PLA, respectively. Despite some variations in structure, the identities and locations of the

catalytic triad were highly conserved, indicating that these enzymes may operate via a similar mechanism. Although the *M. musculus* catalytic residues exhibited subtle differences in position, they possessed a similar orientation in the active site pocket.

PflCAT-PLA catalyzes the hydrolysis of PC at both *sn*-1 and *sn*-2 positions and preferentially catalyzes the hydrolysis of *sn*-2-ricinoleoyl-PC over *sn*-2-18:1-PC

To characterize its enzymatic properties, PflCAT-PLA, heterologously produced in yeast, was subjected to nickel-NTA affinity purification (Figure S2) and the resulting partially purified enzyme was used in subsequent assays. The soluble nature of PflCAT-PLA was consistent with previous observations on AtLCAT-PLA (Chen *et al.*, 2012). PflCAT-PLA catalyzed the hydrolysis of acyl groups at both *sn*-1 and *sn*-2 positions of 18:1-PC and Ric-PC. Interestingly, this enzyme preferentially catalyzed the hydrolysis of the *sn*-2-oleoyl chain over the *sn*-1-palmitoyl chain of 18:1-PC, but displayed a slightly higher activity towards the *sn*-1-palmitoyl chain than the *sn*-2-ricinoleoyl chain of Ric-PC (Figure 3a). The PLA₁ and PLA₂ activities of PflCAT-PLA were further analyzed using increasing bulk concentrations of 18:1-PC or Ric-PC (Figure 3b–e). Both PLA₁ and PLA₂ activities showed a similar response to increasing bulk concentrations of both PCs, whereby maximum enzymatic activity was achieved at approximately 45 μ M PC. The PLA₁ and PLA₂ activity data for PflCAT-PLA showed better fits to the allosteric sigmoidal equation over the Michaelis–Menten equation with Hill coefficient values of 2.27–2.60. It should be noted that PflCAT-PLA displayed similar apparent enzymatic kinetics towards the *sn*-1-palmitoyl chain of 18:1-PC and the *sn*-1-palmitoyl chain of Ric-PC (Figure 3c,e), suggesting that the acyl chain on the *sn*-2 position of PC may have little effect on PLA₁ activity. Conversely, the apparent V_{\max} value of PflCAT-PLA towards the *sn*-2-oleoyl chain of 18:1-PC was two-fold higher than that towards the *sn*-2-ricinoleoyl chain of Ric-PC (Figure 3b,d), which indicates that PflCAT-PLA displayed higher specificity towards 18:1-PC than to Ric-PC.

To examine the substrate specificity of PflCAT-PLA towards the *sn*-2 position of phospholipids, various substrates including 18:1-PC, Ric-PC, *sn*-1-palmitoyl-*sn*-2-linoleoyl-PC (18:2-PC), and *sn*-1-palmitoyl-*sn*-2-linoleoyl-phosphatidylethanolamine (18:2-PE) were supplied at equal amounts in separate assays. *Physaria* LCAT-PLA was able to use all tested PCs and PE (Figure 4a), but appeared to prefer PC over PE and displayed the highest activity towards 18:1-PC, followed by Ric-PC, 18:2-PC and finally 18:2-PE (Figure 4a). Consistent with previous enzyme assay results (Figure 3b,d), the activity of PflCAT-PLA for 18:1-PC was about two-fold higher than for Ric-PC (Figure 4a). Subsequently, the substrate selectivity of PflCAT-PLA, RcLCAT-PLA or AtLCAT-PLA for 18:1-PC or Ric-PC at the

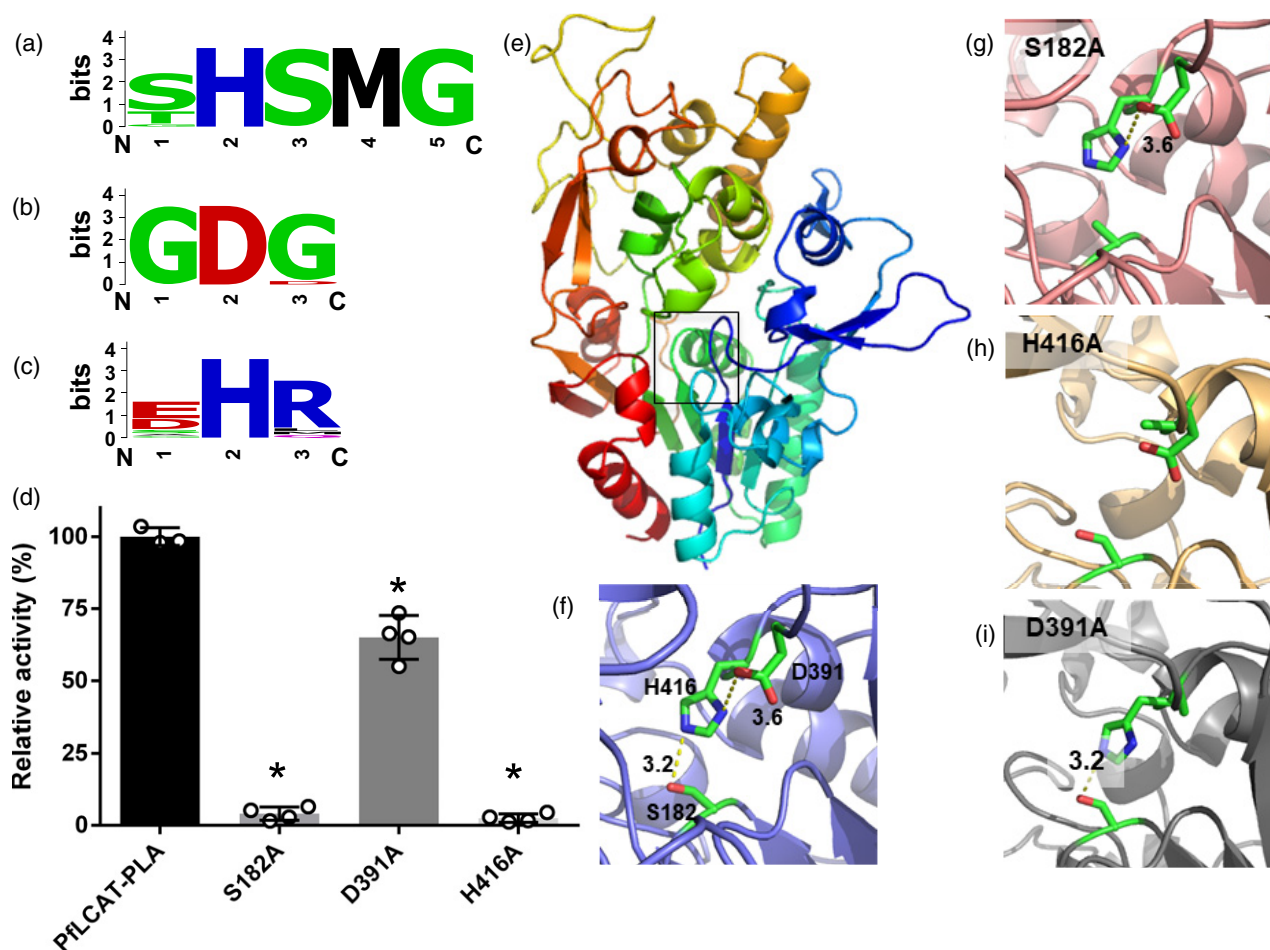


Figure 2. *Physaria fendleri* lecithin:cholesterol acyltransferase-like phospholipase A (PflCAT-PLA) contains a conserved Ser/Asp/His catalytic triad, whose mutation dramatically affects the enzyme activity.

(a)–(c) Sequence logo showing the conserved nature of the catalytic triad of LCAT-PLA, including Ser (A), Asp (b) and His (c). (d) Enzyme activity of PflCAT-PLA and its mutants S182A, D391A and H416A using crude yeast recombinant proteins and $45 \mu\text{M}$ of 1-palmitoyl-2- ^{14}C oleoyl-phosphatidylcholine. The activity of recombinant PflCAT-PLA was set as 100%. Data represent mean \pm SD ($n = 3$ for PflCAT-PLA; $n = 4$ for its mutants). Asterisks indicate a significant difference in activity between the recombinant wild-type enzyme and mutant enzymes (t -test, $P < 0.05$). (e) Homology model of PflCAT-PLA obtained using SWISS-MODEL software. (f)–(i) Close-up view of the active site pockets of wild-type PflCAT-PLA and its mutants S182A, H416A and D391A.

sn-2 position was examined by mixing both PC species at equimolar ratios ($22.5 \mu\text{M}$ each) in each assay. All three plant LCAT-PLAs showed higher selectivity for the *sn*-2-oleoyl chain of Ric-PC than the *sn*-2-oleoyl chain of 18:1-PC (Figure 4b), with RcLCAT-PLA and PflCAT-PLA displaying 3.3- and 2.3-fold higher activity with Ric-PC than 18:1-PC, respectively, and AtLCAT-PLA exhibiting 1.5-fold higher activity for Ric-PC than 18:1-PC (Figure 4b). Taken together, the results of these *in vitro* assays suggest that PflCAT-PLA and RcLCAT-PLA contribute to the turnover of PC by preferentially cleaving *sn*-2-ricinoleoyl chains.

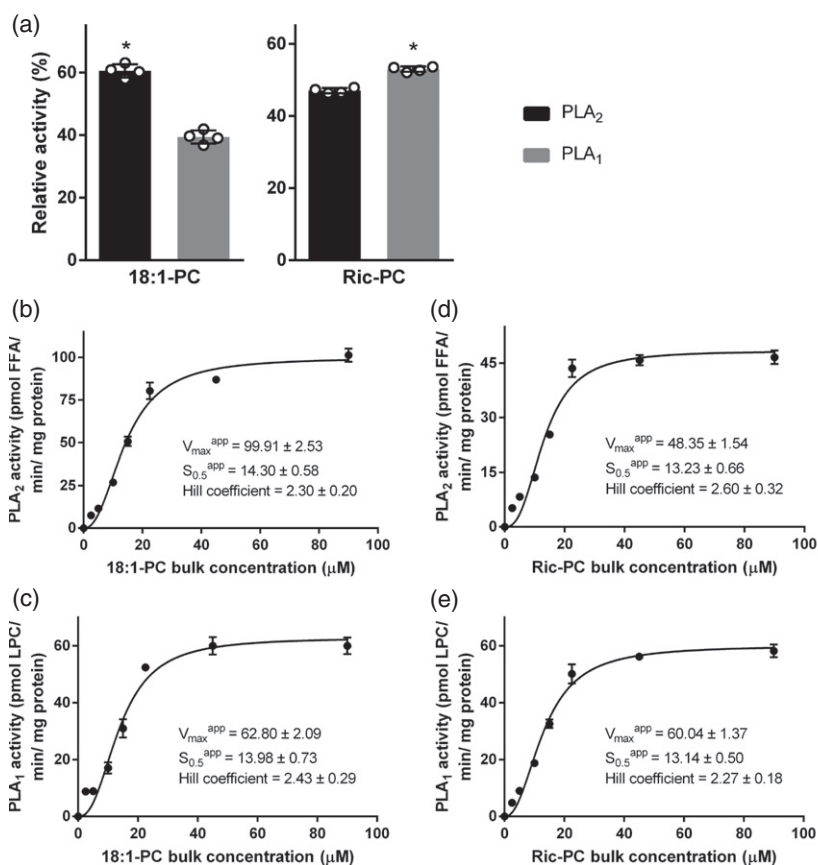
PflCAT-PLA and RcLCAT-PLA are expressed constitutively with relatively high transcript levels in roots and developing seeds

The expression of PflCAT-PLA was assessed in different tissues using quantitative real-time reverse transcription PCR

(qRT-PCR) and results indicated that PflCAT-PLA was expressed in all tissues tested, including roots, stems, leaves, flowers and developing siliques at different developmental stages (Figure 5). The highest levels of expression were observed in PflCAT-PLA roots, followed by developing siliques at 19, 17 and 10–14 days after pollination (DAP). Confirmation of the qRT-PCR results was achieved through the generation of transgenic Arabidopsis lines bearing a cassette in which the PflCAT-PLA promoter was fused to the β -GLUCURONIDASE (*uidA*) reporter gene [Figure 6; promoterless control of β -GLUCURONIDASE protein (GUS) staining is shown in Figure S3]. As expected, these lines exhibited GUS staining in various tissues and organs, with the exception of trichomes, where no staining was observed. Embryos displayed strong GUS staining in the mid-stages of silique development, while staining appeared to be absent in mature siliques. High levels of staining were

Figure 3. *Physaria fendleri* lecithin:cholesterol acyl-transferase-like phospholipase A (PflCAT-PLA) displays phospholipase A₁ and A₂ activities.

(a) PflCAT-PLA catalyzes the hydrolysis of *sn*-1-palmitoyl-*sn*-2-[¹⁴C] ricinoleoyl-phosphatidylcholine (Ric-PC) or *sn*-1-palmitoyl-*sn*-2-[¹⁴C] oleoyl-PC (18:1-PC) at both *sn*-1 and *sn*-2 positions. Enzyme activity was assessed using 45 μ M of Ric-PC or 18:1-PC. (b), (c) Phospholipase A₁ (PLA₁) and PLA₂ activities of PflCAT-PLA in response to increasing 18:1-PC concentrations from 2.5 to 90 μ M. FFA, free fatty acid. (d), (e) PLA₁ and PLA₂ activities of PflCAT-PLA in response to increasing Ric-PC concentrations from 2.5 to 90 μ M. LPC, lysophosphatidylcholine. Data were fitted to the allosteric sigmoidal equation using GraphPad Prism. In (a) asterisks indicate significant differences between the relative PLA₁ and PLA₂ activities (*t*-test, *P* < 0.05). Data represent mean \pm SD (*n* = 4).



also noted in roots, leaves and developing siliques. In floral tissues, GUS staining was mainly observed in anthers and stigmas, while there was little GUS staining in petals.

Relatively high levels of *LCAT-PLA* expression in the developing seeds/endosperm of *Physaria* and *castor* were also observed in previously released transcriptome data (Troncoso-Ponce *et al.*, 2011; Horn *et al.*, 2016). From these data, *LCAT-PLAs* were shown to make up a large component of total *PLA* expression in the developing seed/endosperm of *Physaria* and *castor*, accounting for 13.9–20.7% and 12.4–50.0% of the total *PLA* transcript abundance, respectively, depending on the stage of development (Figure S4). Taken together, these results suggest a possible role for the encoded PflCAT-PLA and RcLCAT-PLA enzymes in catalyzing the removal of HFAs from PC in developing seeds of *castor* and *Physaria*.

Expression of PflCAT-PLA or RcLCAT-PLA with RcFAH12 increases the proportion of hydroxy fatty acid at the *sn*-1/3 positions of triacylglycerol in the seeds of transgenic Arabidopsis

To gain insight into the possible role of *LCAT-PLAs* in seed oil formation, cDNA encoding PflCAT-PLA, RcLCAT-PLA or AtLCAT-PLA was fused to the seed-specific *Napin* promoter and transformed into the Arabidopsis CL7 line (bearing an *RcFAH12* over-expression cassette in an *fae1*

mutant background; Kunst *et al.*, 1992; Lu *et al.*, 2006). Transgenic T₂ seeds, along with untransformed CL7 control seeds, were then subjected to in-depth seed oil analyses. None of the transgenic Arabidopsis lines expressing any of the three *LCAT-PLAs* exhibited significant alterations in total seed lipid content when compared with the CL7 control lines (Figure 7a). In CL7 lines, HFA made up 14.87 \pm 2.78% of total fatty acids, while PflCAT-PLA and RcLCAT-PLA over-expressing lines accumulated 17.21 \pm 0.66% and 17.07 \pm 0.78% HFAs in their seeds, respectively; increases that were not significantly higher than the CL7 control lines (Figure 7b, Table S1). In contrast, AtLCAT-PLA over-expressing lines exhibited HFA (14.05 \pm 1.42%) levels that were similar to those seen in CL7 control lines (Figure 7b). To examine the distribution of HFAs in polar and neutral lipids, total lipids from mature T₂ seeds of CL7 control and transgenic Arabidopsis lines were separated on TLC plates into polar lipid and TAG fractions. In the seeds of the PflCAT-PLA and RcLCAT-PLA over-expressing lines, HFA content within the TAG and polar lipid fractions was slightly, but insignificantly, increased compared with control CL7 lines (Figure 7c, Table S2). In contrast, AtLCAT-PLA over-expressing lines showed a slight but insignificant decrease in HFA content in TAG, and no significant difference in polar lipid fractions (Figure 7c, Table S2). A TAG positional analysis was also

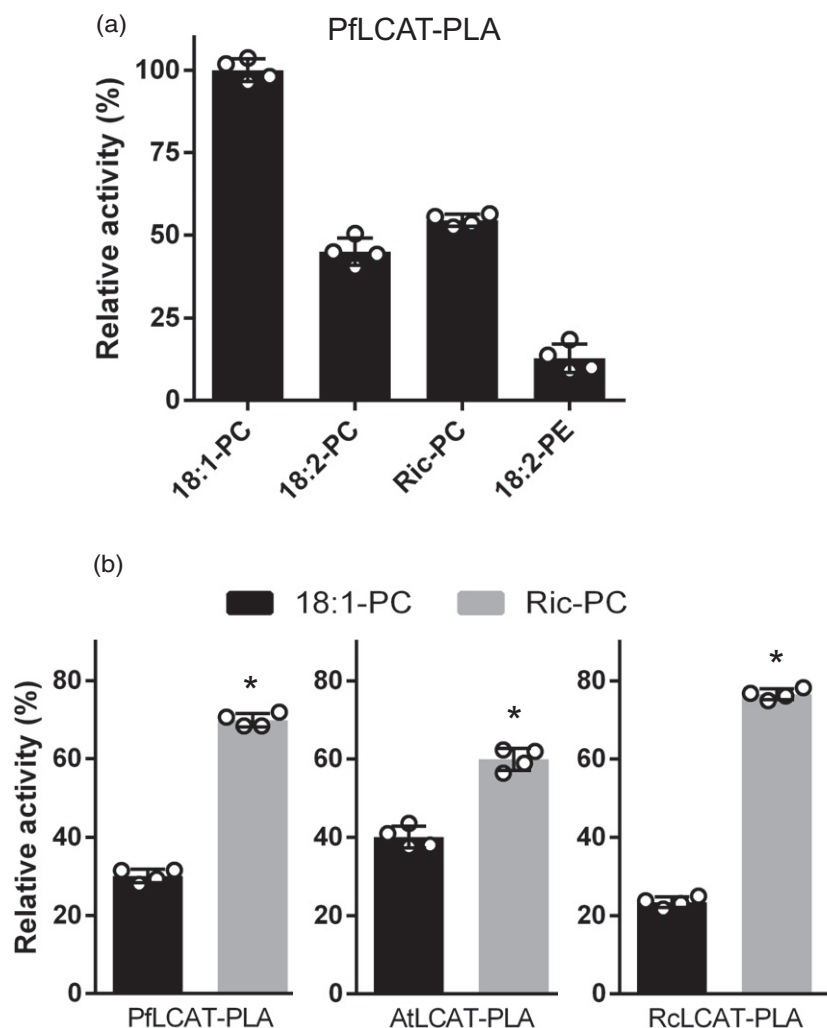


Figure 4. Lecithin:cholesterol acyltransferase-like phospholipase A (LCAT-PLA) from *Physaria*, castor or *Arabidopsis* preferentially catalyzes the hydrolysis of *sn*-1-palmitoyl-*sn*-2-[14 C] ricinoleoyl-phosphatidylcholine (Ric-PC) over *sn*-1-palmitoyl-*sn*-2-[14 C] oleoyl-PC (18:1-PC).

(a) Substrate specificity of PfLCAT-PLA towards Ric-PC, 18:1-PC, *sn*-2-[14 C] linoleoyl-PC (18:2-PC) and *sn*-2-[14 C] linoleoyl-phosphatidylethanolamine (18:2-PE). Enzyme activity was assessed using 45 μ M of Ric-PC, 18:1-PC, 18:2-PC or 18:2-PE.

(b) Substrate selectivity of PfLCAT-PLA, RcLCAT-PLA and AtLCAT-PLA towards Ric-PC and 18:1-PC. Equal amounts of 18:1-PC and Ric-PC (22.5 μ M each) were mixed and used in the assay. Asterisks indicate significant differences between the activities towards Ric-PC and 18:1-PC (*t*-test, $P < 0.05$). Data represent mean \pm SD ($n = 4$).

conducted to determine the regiospecific distribution of HFAs in TAG. Over-expression of *PfLCAT-PLA* or *RcLCAT-PLA* but not *AtLCAT-PLA* increased the proportion of HFAs at *sn*-1/3 positions (Figure 7d), which was accompanied by concomitant and significant decreases in 18:2 at these positions (Table S3).

DISCUSSION

In recent years, interest in utilizing transgenic plants to produce valuable lipids, such as HFAs, has gained momentum since plants that naturally accumulate them are not suitable for large-scale agriculture. The expression of *RcFAH12* in *Arabidopsis* seeds has been shown to lead to HFA accumulation of up to 11% of total fatty acids in PC, which is two-fold higher than that in castor and represents a bottleneck for HFA production in *Arabidopsis* seed TAG (Bates and Browse, 2011; van Erp *et al.*, 2011). These findings suggest that the endogenous *Arabidopsis* enzymes are unable to efficiently remove HFAs from the *sn*-2 position of PC, which is the site of HFA biosynthesis. In plants,

enzymes from three PLA families, including sPLA₂, pPLA and LCAT-PLA, have been reported to catalyze the liberation of fatty acids from the *sn*-2 (or both *sn*-1 and *sn*-2) position of PC (Li *et al.*, 2011; Chen *et al.*, 2012; Bayon *et al.*, 2015) and specialized versions of these enzymes in HFA-accumulating plants may contribute to HFA turnover in PC. While both castor sPLA₂ α and pPLAIII have been shown to facilitate the removal of HFAs from PC in transgenic *Arabidopsis* *RcFAH12/fae1* lines, the resulting HFA was not efficiently incorporated into TAG (Bayon *et al.*, 2015; Lin *et al.*, 2019). Since the function of LCAT-PLAs in acyl editing has yet to be explored, the current study aimed to identify and functionally characterize homologs from *Physaria* and castor as a means of assessing their role in HFA turnover on PC and potentially distinguishing further candidates for the downstream manipulation of unusual fatty acid production in transgenic plants.

A single LCAT-PLA homolog was identified in *Physaria* and castor, respectively, and phylogenetic analysis indicated that plant LCAT-PLAs grouped with LCAT-PLA₁

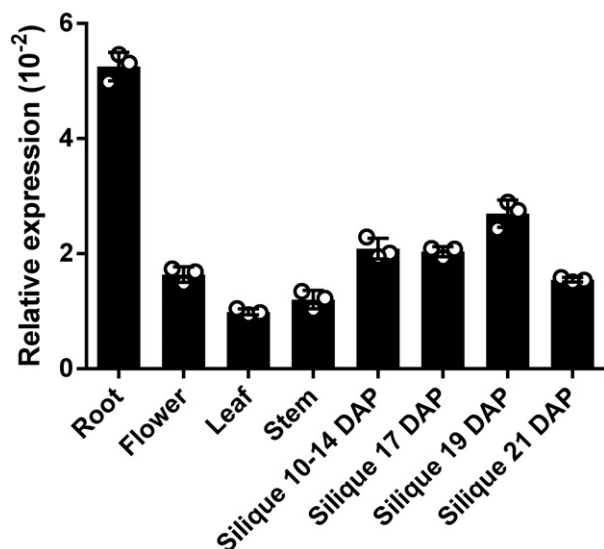


Figure 5. *Physaria fendleri* lecithin:cholesterol acyltransferase-like phospholipase A (*PflCAT-PLA*) is expressed throughout *Physaria fendleri* development.

Quantitative real-time RT-PCR analysis of *PflCAT-PLA* expression in various *P. fendleri* tissues and developmental stages, including root, stem, leaf, floral tissue and siliques at 10–14, 17, 19 and 21 days after pollination (DAP). Data represent means of the relative *PflCAT-PLA* transcript ($2^{-\Delta CT}$) from three replicates \pm SD with *18S rRNA* as the internal reference gene.

proteins, which are closely related to LCAT, animal LPLA₂, PDAT and PSAT proteins (Figure 1). The conserved signature motifs of plant LCAT-PLAs and their close homologs include a lipase motif (XHSXG) containing the catalytic Ser of the active site, as well as a catalytic triad (Ser/Asp/His) (Figures 1, 2a–c, and S1). The importance of the catalytic triad was confirmed by site-directed mutagenesis, whereby mutation of Ser182, Asp391 or His416 to Ala in *PflCAT-PLA* dramatically decreased enzyme activity (Figure 2d), probably due to disruption of the catalytic nucleophile (Figure 2e–i).

Unlike the previously characterized *Arabidopsis* LCAT-PLA₁ with *sn*-1 regio-specificity of PC (Noiriel *et al.*, 2004), the *in vitro* assays implemented in this current study suggested that *PflCAT-PLA* is able to catalyze the hydrolysis of fatty acyl chains at both the *sn*-1 and *sn*-2 positions of PC (Figure 3), which is consistent with our previous results with *AtLCAT-PLA* (Chen *et al.*, 2012). The substrate saturation plots of both PLA₁ and PLA₂ activities of *PflCAT-PLA* showed a sigmoidal response (Figure 3b–e), which is similar to the kinetic behavior of many other phospholipases (Hendrickson and Dennis, 1984a,b; Burke *et al.*, 1995; Merkel *et al.*, 1999). This sigmoidal behavior may indicate that the enzyme requires more than one PC molecule to interact with to induce a conformational change for activation (Hendrickson and Dennis, 1984a,b). Indeed, interfacial activation is widely present in many lipases as a means of facilitating a switch from closed to open conformations in

response to lipid binding (Mouchlis *et al.*, 2014). In line with this, a lid region and a membrane-binding domain have been identified in mammalian LPLA₂, which is a close homolog of LCAT-PLA, although no solid evidence for a large conformational change upon membrane binding has yet been reported (Glukhova *et al.*, 2015).

It has been suggested that PLAs may contribute to the selective transfer of HFAs from the *sn*-2 position of PC to TAG (Bayon *et al.*, 2015; Lin *et al.*, 2019) but so far the specifics of this process remain elusive. Although castor sPLA₂ α has been shown to be more efficient at catalyzing the hydrolysis of Ric-PC than *Arabidopsis* sPLA₂ α , this enzyme displayed higher specificity and selectivity for 18:1-PC than Ric-PC (Bayon *et al.*, 2015). In the current study, enzyme assay data indicated that both *PflCAT-PLA* and *RcLCAT-PLA* exhibited increased selectivity for Ric-PC over 18:1-PC in the presence of mixed substrates (Figure 4b), although the enzymes showed a higher specificity for 18:1-PC than Ric-PC (Figure 4a). Increased selectivity for Ric-PC over 18:1-PC was also observed for *AtLCAT-PLA*, but to a smaller degree than for *PflCAT-PLA* or *RcLCAT-PLA* (Figure 4b). Different enzymatic properties with respect to substrate specificity and selectivity have also been reported for other enzymes. For example, *Brassica napus* diacylglycerol acyltransferase (DGAT) 1, which exhibited four- to seven-fold higher specificity for 16:0-CoA over 18:1-CoA in substrate specificity assays, incorporated two- to five-fold higher amounts of 18:1 than 16:0 in substrate selectivity assays with 18:1-CoA and 16:0-CoA in a 3:1 ratio (Aznar-Moreno *et al.*, 2015). Moreover, qRT-PCR and GUS fusion results both indicated that *PflCAT-PLA* is expressed at relatively high levels in developing seeds (Figures 5 and 6), and analysis of previously released transcriptome data revealed that *LCAT-PLAs* make up a substantial proportion of *PLA* transcripts in castor and *Physaria* (Figure S4), which supports the possible involvement of LCAT-PLAs in HFA enrichment in plants producing hydroxy seed oils. Taken together, *PflCAT-PLA* or *RcLCAT-PLA* may be more effective than *AtLCAT-PLA* in catalyzing the hydrolysis of Ric-PC, and thus may contribute to turnover of HFA in PC. Further *in vitro* and *in vivo* studies of LCAT-PLAs will be necessary to explore their enzymatic properties and physiological roles in this context. Additionally, *PflCAT-PLA* is also expressed in other tissues, with roots being the highest (Figure 5). Previously, different PLAs have been shown to function in root development through the release of free fatty acids and LPC or lysophosphatidylethanolamine signaling molecules (Lee *et al.*, 2010; Rietz *et al.*, 2010). Considering that *PflCAT-PLA* is able to utilize different substrates in addition to Ric-PC (Figure 4a), which is not present in non-seed tissues, *PflCAT-PLA* may have currently unknown physiological functions in these tissues. It will also be interesting to probe the potential structural differences between *PflCAT-PLA* and *AtLCAT-*

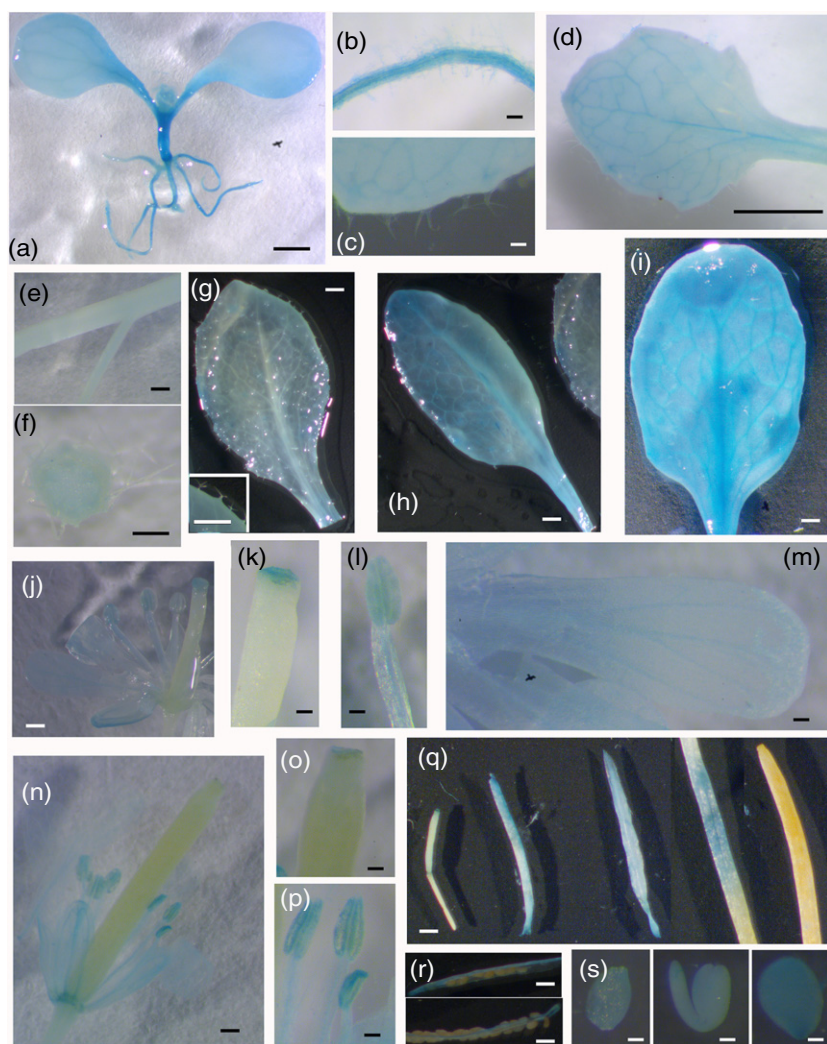


Figure 6. Beta-glucuronidase staining of transgenic *PflCAT-PLA-uidA* transcriptional fusion Arabidopsis lines.

The promoter region of the *Physaria* lecithin:cholesterol acyltransferase-like phospholipase A (*LCAT-PLA*) gene was fused to a *uidA* reporter gene then stably expressed in transgenic Arabidopsis. Tissues include a young seedling (a), root and root hair of young seedling (b), first leaf and trichome of young seedling (c), first leaf of young seedling (d), stem long-section (e), stem cross-section (f), young rosette leaf and trichome (g), middle rosette leaf (h), old rosette leaf (i), young flower (j), stigma of young flower (k), anther and filament of young flower (l), petal of young flower (m), mature flower (n), stigma of mature flower (o), anther and filament of mature flower (p), developing silique at different stages (q), cut silique (r) and developing seeds and embryo (s). Pictures are representative of at least 16 independent T_1 lines. For (a), (d), (e)–(j), (n), (q) and (r) scale bars = 1 mm; for (b), (c), (k)–(m), (o), (p) and (s) scale bars = 0.1 mm.

PLA based on the derived structural models. However, no homologous enzyme has been crystallized in the presence of a phospholipid substrate to date, making it difficult to make reliable speculation on the structural basis of the preference of *PflCAT-PLA* for HFA-containing PC.

Recently, both castor *sPLA₂α* and *pPLAIII* were shown to be able to efficiently remove HFAs from PC in corresponding transgenic Arabidopsis lines, but the cleaved HFAs failed to be incorporated into TAG as shown by dramatic decreases of HFA content in seed oil (Bayon *et al.*, 2015; Lin *et al.*, 2019). Interestingly, the current study shows that over-expressing *PflCAT-PLA*, *RcLCAT-PLA* or *AtLCAT-PLA* in Arabidopsis CL7 lines (over-expressing *RcFAH12* in an *fae1* mutant background) did not significantly affect total lipid content and HFA accumulation within seed oil compared with untransformed CL7 lines (Figure 7). More importantly, the over-expression of *PflCAT-PLA* or *RcLCAT-PLA* increased the proportion of HFAs on the *sn*-1/3 positions of TAG (Figure 7d), despite there being only

small but insignificant increases in HFA accumulation in TAG and polar lipid fractions being noted (Figure 7c). This probably resulted from an increase in the efficiency of HFA removal at the *sn*-2 position of PC, and the subsequent incorporation of HFA into *sn*-1/3 positions of TAG catalyzed by other enzymes such as *sn*-glycerol-3-phosphate acyltransferase (GPAT) and DGAT. Since the most rapid PC and TAG exchange appears to occur during mid-stages of seed development, further analysis of HFA distribution in PC and TAG in developing seeds may provide more information on the effect of *LCAT-PLA* on PC turnover, representing an interesting future direction for research. On the other hand, *AtLCAT-PLA* had no effect on HFA distribution in TAG (Figure 7d), although it also preferred Ric-PC over 18:1-PC *in vitro* (Figure 4).

While over-expression of *PflCAT-PLA* or *RcLCAT-PLA* was able to enrich the HFA content at the *sn*-1/3 positions of TAG compared with CL7 controls, the final HFA content within total seed oil and seed TAG only reached about

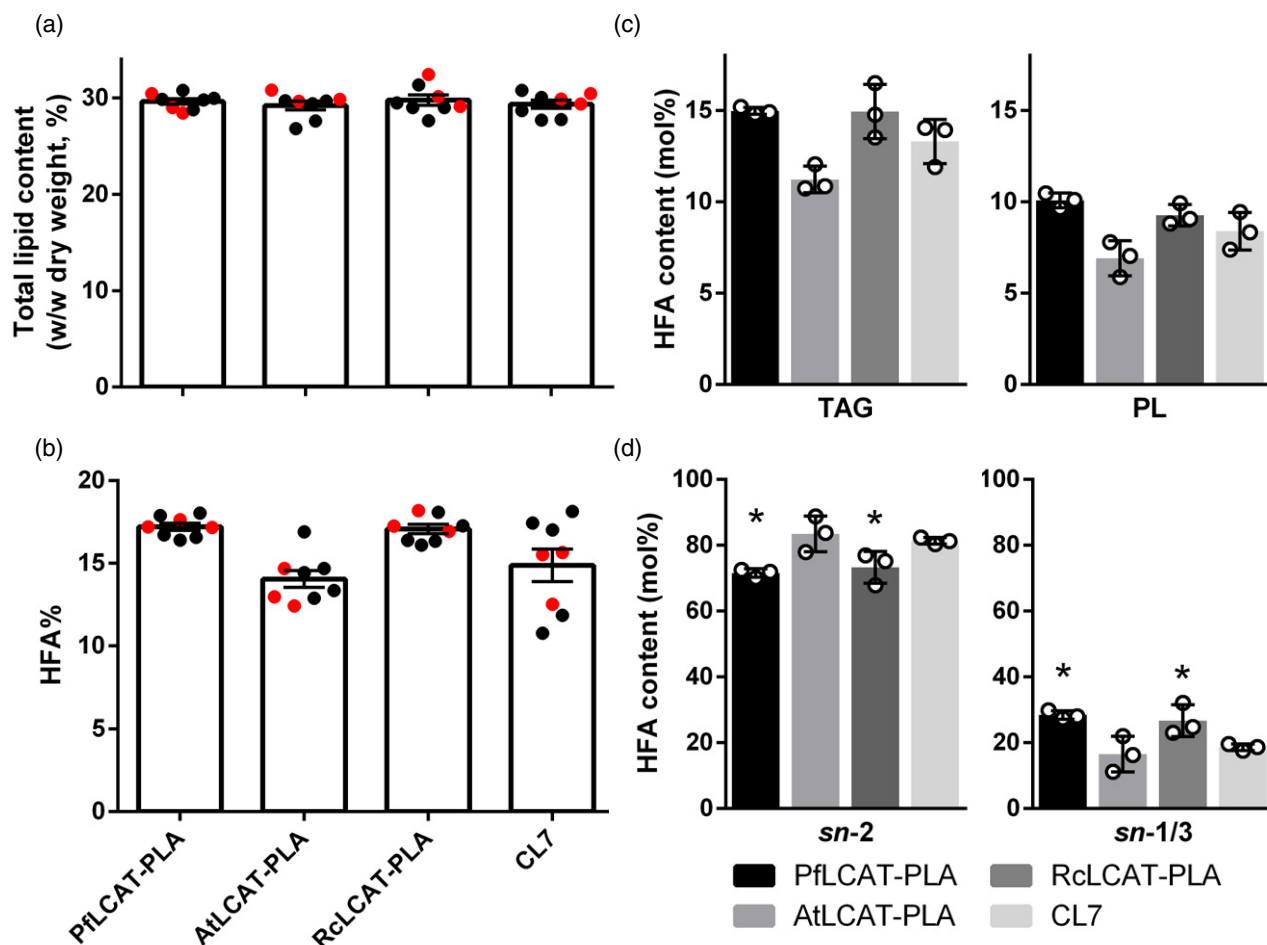


Figure 7. Over-expression of *Physaria fendleri* lecithin:cholesterol acyltransferase-like phospholipase A (*PfLCAT-PLA*) or castor *LCAT-PLA* affects the stereochemical position of hydroxy fatty acids (HFAs) in lipids of transgenic Arabidopsis CL7 lines.

(a) Total lipid content in the seed oil of T₂ seeds of transgenic Arabidopsis CL7 lines.

(b) The HFA content in the T₂ seeds of transgenic Arabidopsis CL7 lines.

(c) The HFA distribution in triacylglycerol (TAG) and phospholipids (PL) from T₂ seeds of transgenic Arabidopsis CL7 lines over-expressing plant *LCAT-PLA*.

(d) Stereochemical position of HFA in TAG. Data represent mean \pm SD. For (a) and (b) $n = 8$ independent transgenic lines; for (c) and (d), $n = 3$ independent transgenic lines (shown as red dots in a and b). Asterisks indicate significant differences in the HFA content of the Arabidopsis over-expressing plant *LCAT-PLA* lines and control lines (t -test, $P < 0.05$).

17.2% (Figure 7). The HFA levels seen in our transgenic lines are much lower than the ricinoleic acid (about 90%) and lesquerolic acid (about 60%) seed TAG contents found in castor and *Physaria*, respectively. Co-expression of multiple enzymes involved in HFA biosynthesis, channeling and incorporation into TAG may be required to elicit these high levels in non-HFA-accumulating oilseed plants. Substrate-selective PLAs, such as LCAT-PLAs, are expected to function together with a long-chain acyl-CoA synthetase (LACS) that preferentially activates HFA to HFA-CoA, which is the active form of fatty acid for further utilization in TAG biosynthesis. The released HFA-CoA can then be utilized by the acyl-CoA-dependent reactions of the Kennedy (1961) pathway of TAG synthesis or captured by acyl-CoA-binding proteins and shuttled towards TAG biosynthesis

(Du *et al.*, 2016; Li-Beisson *et al.*, 2017). While the previous co-expression of castor *LACSs* with *sPLA₂ α* in transgenic Arabidopsis *RcFAH12/FAE1* lines did not increase HFA accumulation in TAG (Bayon *et al.*, 2015), it may be that HFAs cleaved by castor *sPLA₂ α* were not efficiently activated to HFA-CoA by the co-produced LACSs. It is also possible that the activated HFA-CoA failed to be transported to the correct subcellular compartment for TAG biosynthesis, potentially due to the lack of an acyl-CoA-binding protein that specifically binds HFA-CoA. The co-expression of cDNAs encoding enzymes in the Kennedy and acyl editing pathways may provide another potential requirement for transferring cleaved HFAs to TAG biosynthesis. Castor and *Physaria* both contain enzymes that contribute to the enrichment of HFA in TAG, probably through enhanced

selectivity for HFA-containing substrates. These include DGAT 1 and 2 (Kroon *et al.*, 2006; McKeon and He, 2015), lysophosphatidic acid acyltransferase (LPAAT) 2 (Chen *et al.*, 2016; Shockey *et al.*, 2019), GPAT9 (Lunn *et al.*, 2019; Shockey *et al.*, 2019), LPCAT (Lager *et al.*, 2013), PDAT (van Erp *et al.*, 2011) and phosphatidylcholine diacylglycerol cholinephosphotransferase (Hu *et al.*, 2012). Considering that these enzymes may form a transferase interactome (Xu *et al.*, 2019), the collective expression of cDNAs encoding multiple transferases may provide even further enhancement in terms of the efficiency of transferring HFAs from PC to TAG. Indeed, the co-expression of castor *GPAT9*, *LPAAT* and *PDAT1* in Arabidopsis *RcFAH12/fae1* lines resulted in the accumulation of HFAs at *sn*-1, -2 and -3 positions of TAG, thus boosting HFA content (Lunn *et al.*, 2019). Additionally, unlike the accumulation of ricinoleic acid (C18-HFA) in castor, Physaria possesses lesquerolic acid (C20-HFA) in its seed oil, which results from the elongation of C18-HFA through the catalytic action of the fatty acid condensing enzyme 3-ketoacyl-CoA synthase 3 (Moon *et al.*, 2001). Thus, the collective expression of any number of genes encoding these additional enzymes, along with *LCAT-PLAs* and *FAH12*, from HFA-accumulating species, is likely to enhance the production of these unusual fatty acids in transgenic oilseed plants.

In conclusion, unique *LCAT-PLAs* have been isolated from Physaria and castor, which display both *PLA*₁ and *PLA*₂ activities and substrate selectivity towards Ric-PC over 18:1-PC. Expression of *PfLCAT-PLA* or *RcLCAT-PLA* in the transgenic *fae1* Arabidopsis over-expressing *RcFAH12* resulted in enrichment of HFAs at the *sn*-1/3 positions of TAG. Taken together, these results suggest that *PfLCAT-PLA* and *RcLCAT-PLA* could contribute to HFA turnover in PC and are potentially useful in engineering HFA production in transgenic plants.

EXPERIMENTAL PROCEDURES

Sequence analysis and protein structure prediction

Multiple sequence alignments of the putative *LCAT-PLA* and *PLA* proteins from different animal and plant species were carried out using the L-INS-i method implemented in the MAFFT web server (<https://mafft.cbrc.jp/alignment/server/>, accessed 4 September 2019) (Katoh and Standley, 2013). The best-fit model for protein alignment (WAG + F + I + G4) was identified using the IQ-TREE web server (<http://iqtree.cibiv.univie.ac.at/>, accessed 4 September 2019) (Trifinopoulos *et al.*, 2016) based on the Bayesian information criterion score. The phylogenetic tree was then constructed with the maximum likelihood method using IQ-TREE and visualized with iTOL v.4 (Letunic and Bork, 2016). The WebLogo server (<https://weblogo.berkeley.edu/logo.cgi>, accessed 4 September 2019) was used to show the sequence logo of the catalytic triad of *LCAT-PLA* from different species, including *Arabidopsis lyrata* (AILCAT-PLA, XP_002867917), *A. thaliana* (AtLCAT-PLA, AF421149, At4g19860; AtLCAT-PLA1, AF421148, At3g03310), *B. rapa* (BrLCAT-PLA, XP_009133245), *Columba livia* (CILCAT-PLA, XP_005512683),

C. sativa (CsLCAT-PLA, XP_010439651), *Chlorella variabilis* (CvLCAT-PLA, XP_005851868), *Glycine max* (GmLCAT-PLA, XP_003529428), *Guillardia theta* (GtLCAT-PLA, XP_005819812), *Medicago truncatula* (MtLCAT-PLA, XP_003607877), *Nicotiana tabacum* (NtLCAT-PLA1, AAQ05032), *P. fendleri* (PfLCAT-PLA, MN817234), *P. patens* (PpLCAT-PLA, XP_001782233), *R. communis* (RcLCAT-PLA, 30060.m000520; RcLCAT-PLA1, 29929.m004538), *Sorghum bicolor* (SbLCAT-PLA, XP_002460515), and *Zea mays* (ZmLCAT-PLA, ACR34350). The structures of *LCAT-PLA* from *P. fendleri*, Arabidopsis, castor, *P. patens* and *M. musculus* were predicted using SWISS-MODEL software with *H. sapiens* LPLA₂ (RCSB 4x92.1) as a template (Glukhova *et al.*, 2015).

Plant growth conditions

Arabidopsis CL7 and other transgenic plants were grown in growth chambers at 22°C with a photoperiod of 18 h day/6 h night and a light intensity of 250 $\mu\text{mol m}^{-2} \text{sec}^{-1}$. The CL7 line contains an *RcFAH12* over-expression cassette in an *fae1* mutant background (Kunst *et al.*, 1992; Lu *et al.*, 2006) and is often used for the production of HFAs of 18 carbons. *P. fendleri* was grown in a growth chamber with a 16 h/8 h day/night cycle at 23°C with 50% relative humidity and a light intensity of 125 $\mu\text{mol m}^{-2} \text{sec}^{-1}$. Plant samples were harvested and snap frozen in liquid nitrogen prior to use.

Isolation of *LCAT-PLA* full-length cDNAs from *P. fendleri* and *R. communis* and mutagenesis of *PfLCAT-PLA*

Total RNA was isolated from *P. fendleri* siliques at 17 DAP using the RNeasy Mini Kit (Qiagen, <https://www.qiagen.com/>). First-strand cDNA was synthesized from total RNA using the QuantiTect Reverse Transcription Kit (Qiagen) according to the manufacturer's instructions. Primers specific to conserved regions of *AtLCAT-PLA* (Ag4g19860) were used to amplify a fraction of the *PfLCAT-PLA*-coding region using *P. fendleri* cDNA as a template. The 5' and 3' ends of the full-length *PfLCAT-PLA*-coding region were amplified using rapid amplification of cDNA ends (RACE) with the GeneRacer Kit (Invitrogen, <https://www.thermofisher.com/>). The full-length coding region of *PfLCAT-PLA* was further amplified from cDNA using primers corresponding to its 5' and 3' ends, and the resulting amplicon was cloned into the pYES2.1/V5-His TOPO yeast expression vector (Invitrogen). Site-directed mutagenesis was used to introduce mutations into the *PfLCAT-PLA* coding sequence through overlapping PCR, and the resulting *PfLCAT-PLA* mutants were ligated into the pYES2.1 vector. The full-length coding sequence of *RcLCAT-PLA* was amplified using a previously generated endospore cDNA library (Chen *et al.*, 2004) as the template and was cloned into the pYES2.1 vector. The stop codon from each sequence was removed for in-frame fusion with a C-terminal V5-His tag. The identity of all sequences was confirmed through sequencing. All primers used in the current study are shown in Table S4.

Heterologous expression of *LCAT-PLAs* in yeast

Constructs containing the native *PfLCAT-PLA*, *RcLCAT-PLA* and *AtLCAT-PLA* (Chen *et al.*, 2012), as well as variant *PfLCAT-PLAs*, were individually transformed into wild-type *Saccharomyces cerevisiae* (Inv Sc1 strain, Invitrogen) using the S.c. EasyComp Transformation Kit (Invitrogen). In brief, yeast transformants were first selected on solid minimal medium [0.67% (w/v) yeast nitrogen base and 0.2% (w/v) synthetic complete medium lacking uracil] containing 2% (w/v) dextrose. Subsequently, the successful transformants were transferred to liquid minimal medium containing 2% (w/v) raffinose, and the resulting cultures were then used to

inoculate minimal medium containing 2% (w/v) galactose and 1% (w/v) raffinose at an initial OD₆₀₀ value of 0.4 for induction of gene expression. The yeast strains were grown at 30°C with shaking at 220 r.p.m., and yeast cells were harvested for enzyme extraction.

Enzyme extraction and partial purification

Crude proteins containing the recombinant LCAT-PLAs were extracted as described previously (Chen *et al.*, 2012). In brief, yeast cells were suspended in 1 ml of lysis buffer containing 50 mM 2-amino-2-(hydroxymethyl)-1,3-propanediol (TRIS)-HCl pH 7.6, 600 mM sorbitol, 1 mM EDTA and 1 mM phenylmethylsulfonyl fluoride and were homogenized with 0.5 mm glass beads using a bead beater (BioSpec Products, <https://biospec.com/>). The crude homogenates were then centrifuged for 10 min at 12 000 *g* at 4°C to remove cell debris and glass beads. The supernatant was further centrifuged at 100 000 *g* at 4°C for 70 min to separate microsome and cytosolic fractions. For partial purification of the recombinant LCAT-PLA proteins, the supernatant was further incubated with Nickel-NTA agarose resin (Thermo Scientific, <https://www.thermofisher.com/>), which was recovered by applying to a fritted glass column, washing and then eluting with 500 mM imidazole. The protein concentration of each sample was determined using the Bradford method (Bradford, 1976).

Phospholipase A assays

The PLA assays were performed as described previously (Chen *et al.*, 2012). In brief, the assay mixture contained 50 mM citrate buffer (pH 5.0), 10 mM CaCl₂, 0.05% Triton X-100, 45 μM of 1-palmitoyl-2-[¹⁴C] oleoyl-PC (18:1-PC; American Radiolabeled Chemicals, <https://www.arcincusa.com/>) and 0.5 μg of purified protein or 30 μg of crude cytosol protein in a total volume of 200 μl. The reaction was initiated by adding crude or partially purified recombinant LCAT-PLA and incubated at 30°C for 4 min before being quenched with 1000 μl of chloroform:methanol (1:1, v/v) and 200 μl of 0.15 M acetic acid. The chloroform phase was recovered by centrifugation, concentrated under a nitrogen stream and then applied onto a TLC plate (0.25 mm silica gel, DC-Fertigplatten, Macherey-Nagel, <https://www.mn-net.com/>). The TLC plate was developed with chloroform:methanol:water:acetic acid (65:25:4:1, v/v/v/v) and the resolved lipids were visualized by phosphorimaging (Typhoon Trio Variable Mode Imager, GE Healthcare, <https://www.gehealthcare.com/>). Spots corresponding to free fatty acids and LPC were scraped and radioactivity was quantified by scintillation counting (LS 6500 multipurpose scintillation counter, Beckman-Coulter, <https://www.beckmancoulter.com/>).

For the substrate specificity assay, 45 μM of 18:1-PC, 1-palmitoyl-2-[¹⁴C] linoleoyl-PC (18:2-PC; American Radiolabeled Chemicals), 1-palmitoyl-2-[¹⁴C] linoleoyl-phosphatidylethanolamine (18:2-PE; American Radiolabeled Chemicals) or 1-palmitoyl-2-[¹⁴C] ricinoleoyl-PC (Ric-PC; synthesized as described by Banaś *et al.* (1992)) was used in each reaction. For the substrate selectivity assay, equal amounts of 18:1-PC and Ric-PC (22.5 μM each) were used in the assay. The reaction was initiated by adding crude or partially purified recombinant LCAT-PLA and incubated at 30°C for 4 min before being quenched with 1000 μl of chloroform:methanol (1:1, v/v) and 200 μl of 0.15 M acetic acid as mentioned above. Reaction mixtures were separated on TLC plates as described previously and the corresponding free fatty acid spots were scraped off, extracted using chloroform (Bligh and Dyer, 1959) and applied onto TLC plates. The TLC plates were then developed with hexane:diethyl ester:acetic acid (50:50:1, v/v/v) to separate oleic acid and ricinoleic acid, and their corresponding spots were scraped off for scintillation counting.

For kinetic studies of purified PflCAT-PLA, enzyme assays were performed using 0.5 μg of partially purified protein and the concentration of [¹⁴C] 18:1-PC or [¹⁴C] Ric-PC was varied from 2.5 to 90 μM. The apparent kinetic parameters were calculated by fitting the data to the Michaelis-Menten or allosteric sigmoidal equation using the program GraphPad Prism version 6.0 (GraphPad Software, <https://www.graphpad.com/>).

Gene expression analysis

Physaria fendleri root, stem, leaf and floral tissue, as well as siliques at 10–14, 17, 19 and 21 DAP were harvested for gene expression analysis. Total RNA extraction and subsequent first-strand cDNA synthesis were carried out using the protocols described in a previous section. Quantitative RT-PCR assays were performed on a 7900HT Fast Real-Time PCR System (Applied Biosystems, <https://www.thermofisher.com/>) using Platinum SYBR Green qPCR master mix (Invitrogen) and 18S rRNA as a reference. The primers utilized for PflCAT-PLA and 18S rRNA amplification are listed in Table S4. Histochemical GUS assays were carried out using various tissues from T₁ transgenic lines bearing the PflCAT-PLA-uidA vector (Singer *et al.*, 2010). Images were collected using an Olympus SZ61 microscope with attached digital camera (Olympus, <https://www.olympus-global.com/>).

Generation of transgenic Arabidopsis

To create a PflCAT-PLA-uidA transcriptional fusion vector for GUS staining, an 1817 bp fragment of the PflCAT-PLA gene, with its 3' end immediately upstream of the transcriptional start codon, was amplified from *P. fendleri* genomic DNA. This fragment was inserted upstream of a cassette comprising the uidA-int sequence (Ohta *et al.*, 1990) and nopaline synthase transcriptional terminator (NOS-t) within the pGreen 0029 background (Hellens *et al.*, 2000). For seed-specific over-expression of LCAT-PLAs, the coding sequences of PflCAT-PLA, AtLCAT-PLA and RcLCAT-PLA, respectively were inserted between the seed-specific Napin promoter and the NOS-t within a modified pZP-RCS1 binary vector (Goderis *et al.*, 2002; Mietkiewska *et al.*, 2014).

All constructs were individually introduced into *Agrobacterium tumefaciens* strain GV3101 via electroporation, and in the case of pGreen-derived vectors the pSOUP helper plasmid (Hellens *et al.*, 2000) was co-transformed. The subsequent *A. tumefaciens*-mediated transformation of the Arabidopsis CL7 line was performed using the floral dip method (Clough and Bent, 1998). T₁ seeds from transformed plants were germinated on selective medium containing kanamycin (50 μg ml⁻¹ in ½ MS medium) and resistant T₁ plants were transferred to soil and grown in growth chambers for GUS staining analysis or to produce T₂ seeds for seed oil analysis. The presence of particular transgenic constructs was confirmed by PCR using DNA extracted from the leaf tissue of T₁ or T₂ lines.

Lipid analysis of Arabidopsis seeds

Total lipid analysis of T₂ seeds was performed using direct transmethylation as described previously (Mietkiewska *et al.*, 2014; Singer *et al.*, 2016). Briefly, after stabilizing seed moisture content in desiccators, approximately 10 mg of seeds were weighed, followed by the addition of 100 μg of triheptadecanoin (C17:0 TAG) internal standard. The seeds were then directly transmethyated through the addition of 2 ml 3N methanolic HCl and incubated for 16 h at 80°C. The resulting fatty acid methyl esters (FAMES) were extracted twice with hexane and analyzed on an Agilent 6890N

Gas Chromatograph (Agilent Technologies, <https://www.agilent.com/>) with a 5975 inert XL Mass Selective Detector or a flame ionization detector as described previously (Mietkiewska *et al.*, 2014; Singer *et al.*, 2016).

For lipid class analysis, total lipids were first extracted from approximately 50 mg of T₂ seeds, and were resolved on TLC plates (Macherey-Nagel) with hexane/ether/acetic acid (50:50:2, v/v/v). Castor oil was loaded in a separate lane as the standard. After visualization by spraying with 0.05% primulin solution (acetone:water, 80:20, v/v), the corresponding TAG and polar lipid spots were scraped into screw cap tubes for transmethylation by incubating in 2 ml 3N methanolic HCl at 80°C for 1 h, and the resulting FAMES were subjected to gas chromatography-mass spectrometry (GC-MS) analysis. For the analysis of fatty acid distribution between *sn*-2 and *sn*-1/3 TAG, TAG spots (containing all TAG molecular species) recovered from the silica gel were extracted twice with diethyl ether, and dried under N₂. One milliliter of 1 mM TRIS-HCl buffer (pH 8.0), 100 µl of 2.2% CaCl₂ and 250 µl of 0.1% deoxycholate were added to each TAG sample, which was then subjected to digestion through the addition of pancreatic lipase (pancreatic lipase type II, Sigma, <https://www.sigmaaldrich.com/>) as described previously (Luddy *et al.*, 1964). The resulting *sn*-2 monoacylglycerol was separated on a silica gel-coated TLC plate with hexane:diethyl ether:acetic acid (70:140:2, v/v/v), visualized with 0.05% primulin solution, and then subjected to transmethylation and GC-MS analysis.

Statistical analysis

Data are shown as mean ± standard deviation. Significant differences between two groups were assessed using Student's *t*-test in Excel software.

ACCESSION NUMBERS

Sequence data from this article can be found in GenBank or Phytozome under the following accession numbers: AtLCAT-PLA, AF421149; PflCAT-PLA, MN817234; RcLCAT-PLA, 30060.m000520.

ACKNOWLEDGEMENTS

This work was supported by the Canada Research Chairs Program (RJW and GC), Natural Sciences and Engineering Research Council of Canada (NSERC) Discovery Grants (RGPIN-2016-05926 to GC and RGPIN-2014-04585 to RJW), Alberta Innovates (GC and RJW), Alberta Agriculture and Forestry (GC), the University of Alberta Start-up Research Grant (GC) and the National Natural Science Foundation of China (grant no. 31371661 to BT). The infrastructure used in this work was funded by the Canadian Foundation for Innovation and Research Capacity Program of Alberta Enterprise and Advanced Education. The authors would like to give special thanks to Dr Sten Stymne (Swedish University of Agricultural Sciences) for valuable comments and discussions on the research project and critical review of the manuscript. We also thank Dr John Browse of Washington State University for kindly providing the Arabidopsis CL7 line, and Pernell Tomasi and Thomas McKeon of US Department of Agriculture-Agricultural Research Service for assistance with *P. fendleri* self-pollinations and the castor cDNA library, respectively. We also thank Mrs Qiyuan Shan of Zhejiang Chinese Medical University for contribution to the GUS staining experiment.

AUTHOR CONTRIBUTIONS

RJW and GC conceptualized, designed and supervised the experiments. GC and YX performed phylogenetic analysis, *in vitro* enzyme assays, gene expression analysis, Arabidopsis transformation, seed lipid assays and data analysis. YX prepared the initial draft of the manuscript with the contribution of GC. KMPC performed partial protein purification and enzyme structure prediction and analysis and contributed to construct generation. SDS designed and generated the constructs for GUS staining and significantly contributed to manuscript editing. EM generated constructs for seed-specific expression of LCAT-PLAs in Arabidopsis. MSG made single-site mutants of PflCAT-PLA. BT contributed to yeast sample preparation and enzymatic analysis. JD, MS, XRZ and QX generated important plant materials, genes and gene libraries and made valuable contribution through discussion. All authors were instrumental in the preparation of the finalized manuscript.

CONFLICT OF INTEREST

The authors declare that they have no conflicts of interest with the content of this article.

DATA AVAILABILITY STATEMENT

All relevant data can be found within the manuscript and its supporting materials.

SUPPORTING INFORMATION

Additional Supporting Information may be found in the online version of this article.

Figure S1. Overlay of the predicted three-dimensional structures of PflCAT-PLA and its homologous from plants and other organisms suggests the highly conserved nature of the Ser/Asp/His catalytic triad.

Figure S2. An SDS-PAGE gel analysis of partially purified *Physaria fendleri* lecithin:cholesterol acyltransferase-like phospholipase A (LCAT-PLA), castor LCAT-PLA and Arabidopsis LCAT-PLA.

Figure S3. Promoterless control of GUS staining.

Figure S4. Relative expression of PHOSPHOLIPASE As in the developing seeds of *Physaria fendleri* and the endosperm of *Ricinus communis*.

Appendix S1. Abbreviations.

Table S1. Fatty acid profile of transgenic Arabidopsis seeds from T₁ lines expressing PflCAT-PLA, RcLCAT-PLA or AtLCAT-PLA in the CL7 background.

Table S2. Fatty acid profile of triacylglycerol and polar lipid fractions from T₂ seeds of transgenic Arabidopsis CL7 lines over-expressing plant LCAT-PLA.

Table S3. Stereochemical position of each fatty acid in triacylglycerol from T₂ seeds of transgenic Arabidopsis CL7 lines over-expressing plant LCAT-PLA.

Table S4. Primers used in the current study.

REFERENCES

- Aznar-Moreno, J., Denolf, P., Van Audenhove, K., De Bodt, S., Engelen, S., Fahy, D., Wallis, J.G. and Browse, J. (2015) Type 1 diacylglycerol acyltransferases of *Brassica napus* preferentially incorporate oleic acid into triacylglycerol. *J. Exp. Bot.* **66**, 6497–6506.
- Badami, R.C. and Kudari, S.M. (1970) Analysis of *Hiptage madablotla* seed oil. *J. Sci. Food Agric.* **21**, 248–249.
- Bafor, M., Smith, M.A., Jonsson, L., Stobart, K. and Stymne, S. (1991) Ricinoleic acid biosynthesis and triacylglycerol assembly in microsomal preparations from developing castor-bean (*Ricinus communis*) endosperm. *Biochem. J.* **280**, 507–514.
- Banaś, A., Johansson, I. and Stymne, S. (1992) Plant microsomal phospholipases exhibit preference for phosphatidylcholine with oxygenated acyl groups. *Plant Sci.* **84**, 137–144.
- Bates, P.D. (2016) Understanding the control of acyl flux through the lipid metabolic network of plant oil biosynthesis. *Biochim. Biophys. Acta Mol. Cell Biol. Lipid.* **1861**, 1214–1225.
- Bates, P.D. and Browse, J. (2011) The pathway of triacylglycerol synthesis through phosphatidylcholine in *Arabidopsis* produces a bottleneck for the accumulation of unusual fatty acids in transgenic seeds. *Plant J.* **68**, 387–399.
- Bates, P.D. and Browse, J. (2012) The significance of different diacylglycerol synthesis pathways on plant oil composition and bioengineering. *Front. Plant Sci.* **3**, 1–11.
- Bates, P.D., Johnson, S.R., Cao, X., Li, J., Nam, J.-W., Jaworski, J.G., Ohlrogge, J.B. and Browse, J. (2014) Fatty acid synthesis is inhibited by inefficient utilization of unusual fatty acids for glycerolipid assembly. *Proc. Natl Acad. Sci. USA*, **111**, 1204–1209.
- Bayon, S., Chen, G., Weselake, R.J. and Browse, J. (2015) A small phospholipase A₂-α from castor catalyzes the removal of hydroxy fatty acids from phosphatidylcholine in transgenic *Arabidopsis* seeds. *Plant Physiol.* **167**, 1259–1270.
- Bligh, E.G. and Dyer, W.J. (1959) A rapid method of total lipid extraction and purification. *Can. J. Biochem. Physiol.* **37**, 911–917.
- Bradford, M.M. (1976) A rapid and sensitive method for the quantitation of microgram quantities of protein utilizing the principle of protein-dye binding. *Anal. Biochem.* **72**, 248–254.
- Broun, P. and Somerville, C. (1997) Accumulation of ricinoleic, lesquerolic, and desinpic acids in seeds of transgenic *Arabidopsis* plants that express a fatty acyl hydroxylase cDNA from castor bean. *Plant Physiol.* **113**, 933–942.
- Burke, J.R., Winner, M.R., Tredup, J., Micanovic, R., Gregor, K.R., Lahiri, J., Trampusch, K.M. and Villafranca, J.J. (1995) Cooperativity and binding in the mechanism of cytosolic phospholipase A₂. *Biochemistry*, **34**, 15165–15174.
- Canonne, J., Froidure-Nicolas, S. and Rivas, S. (2011) Phospholipases in action during plant defense signaling. *Plant Signal. Behav.* **6**, 13–18.
- Chapman, K.D. and Ohlrogge, J.B. (2012) Compartmentation of triacylglycerol accumulation in plants. *J. Biol. Chem.* **287**, 2288–2294.
- Chen, G. (2016) Lesquerella (*Physaria* spp.). In *Industrial Oil Crops*. (McKeon, T.A., Hayes, D.G., Hildebrand, D.F. and Weselake, R.J., eds). New York/Urba: Elsevier/AOCS Press, pp. 313–315.
- Chen, G.Q., van Erp, H., Martin-Moreno, J., Johnson, K., Morales, E., Browse, J., Eastmond, P.J. and Lin, J.T. (2016) Expression of castor *LPAT2* enhances ricinoleic acid content at the sn-2 position of triacylglycerols in lesquerella seed. *Int. J. Mol. Sci.* **17**, 1–14.
- Chen, G., Greer, M.S., Lager, I., Yilmaz, J.L., Mietkiewska, E., Carlsson, A.S., Stymne, S. and Weselake, R.J. (2012) Identification and characterization of an LCAT-like *Arabidopsis thaliana* gene encoding a novel phospholipase A. *FEBS Lett.* **586**, 373–377.
- Chen, G.Q., He, X., Liao, L.P. and McKeon, T.A. (2004) 2S albumin gene expression in castor plant (*Ricinus communis* L.). *J. Am. Oil. Chem. Soc.* **81**, 867–872.
- Chen, G., Snyder, C.L., Greer, M.S. and Weselake, R.J. (2011) Biology and biochemistry of plant phospholipases. *Crit. Rev. Plant Sci.* **30**, 239–258.
- Clough, S.J. and Bent, A.F. (1998) Floral dip: a simplified method for *Agrobacterium*-mediated transformation of *Arabidopsis thaliana*. *Plant J.* **16**, 735–743.
- Du, Z.Y., Arias, T., Meng, W. and Chye, M.L. (2016) Plant acyl-CoA-binding proteins: an emerging family involved in plant development and stress responses. *Prog. Lipid Res.* **63**, 165–181.
- van Erp, H., Bates, P.D., Burgal, J., Shockey, J. and Browse, J. (2011) Castor phospholipid:diacylglycerol acyltransferase facilitates efficient metabolism of hydroxy fatty acids in transgenic *Arabidopsis*. *Plant Physiol.* **155**, 683–693.
- Falarz, L., Xu, Y., Caldo, K., Garraway, C., Singer, S. and Chen, G. (2020) Characterization of the diversification of phospholipid:diacylglycerol acyltransferases in the green lineage. *Plant J.* **103**, 2025–2038.
- Glukhova, A., Hinkovska-Galcheva, V., Kelly, R., Abe, A., Shayman, J.A. and Tesmer, J.J. (2015) Structure and function of lysosomal phospholipase A₂ and lecithin:cholesterol acyltransferase. *Nat. Commun.* **6**, 6250.
- Goderis, I.J.W.M., De Bolle, M.F.C., François, I.E.J.A., Wouters, P.F.J., Broekaert, W.F. and Cammue, B.P.A. (2002) A set of modular plant transformation vectors allowing flexible insertion of up to six expression units. *Plant Mol. Biol.* **50**, 17–27.
- Hellens, R.P., Anne Edwards, E., Leyland, N.R., Bean, S. and Mullineaux, P.M. (2000) pGreen: A versatile and flexible binary Ti vector for *Agrobacterium*-mediated plant transformation. *Plant Mol. Biol.* **42**, 819–832.
- Hendrickson, H.S. and Dennis, E.A. (1984a) Analysis of the kinetics of phospholipid activation of *cobra venom* phospholipase A₂. *J. Biol. Chem.* **259**, 5740–5744.
- Hendrickson, H.S. and Dennis, E.A. (1984b) Kinetic analysis of the dual phospholipid model for phospholipase A₂ action. *J. Chem. Inf. Model.* **259**, 5734–5739.
- Horn, P.J., Liu, J., Cocuron, J.C., McGlew, K., Thrower, N.A., Larson, M., Lu, C., Alonso, A.P. and Ohlrogge, J. (2016) Identification of multiple lipid genes with modifications in expression and sequence associated with the evolution of hydroxy fatty acid accumulation in *Physaria fendleri*. *Plant J.* **86**, 322–348.
- Hu, Z., Ren, Z. and Lu, C. (2012) The phosphatidylcholine diacylglycerol cholinephosphotransferase is required for efficient hydroxy fatty acid accumulation in transgenic *Arabidopsis*. *Plant Physiol.* **158**, 1944–1954.
- Katoh, K. and Standley, D.M. (2013) MAFFT multiple sequence alignment software version 7: Improvements in performance and usability. *Mol. Biol. Evol.* **30**, 772–780.
- Kennedy, E. (1961) Biosynthesis of complex lipids. *Fed. Proc.* **20**, 934–940.
- Kim, H.J., Ok, S.H., Bahn, S.C., Jang, J., Oh, S.A., Park, S.K., Twell, D., Ryu, S.B. and Shin, J.S. (2011) Endoplasmic reticulum- and Golgi-localized phospholipase A₂ plays critical roles in *Arabidopsis* pollen development and germination. *Plant Cell*, **23**, 94–110.
- Kroon, J.T.M., Wei, W., Simon, W.J. and Slabas, A.R. (2006) Identification and functional expression of a type 2 acyl-CoA:diacylglycerol acyltransferase (*DGAT2*) in developing castor bean seeds which has high homology to the major triglyceride biosynthetic enzyme of fungi and animals. *Phytochemistry*, **67**, 2541–2549.
- Kunst, L., Taylor, D. and Underhill, E. (1992) Fatty acid elongation in developing seeds of *Arabidopsis thaliana*. *Plant Physiol. Biochem.* **30**, 425–434.
- Lager, I., Yilmaz, J.L., Zhou, X.-R. et al. (2013) Plant acyl-CoA:lysophosphatidylcholine acyltransferases (LPCATs) have different specificities in their forward and reverse reactions. *J. Biol. Chem.* **288**, 36902–36914.
- Lands, W. (1960) Metabolism of glycerolipids: II. The enzymatic acylation of lysolecithin. *J. Biol. Chem.* **235**, 2233–2237.
- Lee, O.R., Kim, S.J., Kim, H.J., Hong, J.K., Ryu, S.B., Lee, S.H., Ganguly, A. and Cho, H.T. (2010) Phospholipase A₂ is required for PIN-FORMED protein trafficking to the plasma membrane in the *Arabidopsis* root. *Plant Cell*, **22**, 1812–1825.
- Letunic, I. and Bork, P. (2016) Interactive tree of life (iTOL) v3: An online tool for the display and annotation of phylogenetic and other trees. *Nucleic Acids Res.* **44**, W242–W245.
- Li-Beisson, Y., Neunzig, J., Lee, Y. and Philippar, K. (2017) Plant membrane-protein mediated intracellular traffic of fatty acids and acyl lipids. *Curr. Opin. Plant Biol.* **40**, 138–146.
- Li, M., Bahn, S.C., Fan, C., Li, J., Phan, T., Ortiz, M., Roth, M.R., Welti, R., Jaworski, J. and Wang, X. (2013) Patatin-related phospholipase pPLAIIIδ increases seed oil content with long-chain fatty acids. *Plant Physiol.* **162**, 39–51.

- Li, M., Bahn, S.C., Guo, L., Musgrave, W., Berg, H., Welti, R. and Wang, X. (2011) Patatin-related phospholipase pPLAIII β -induced changes in lipid metabolism alter cellulose content and cell elongation in *Arabidopsis*. *Plant Cell*, **23**, 1107–1123.
- Li, M., Wei, F., Tawfall, A., Tang, M., Saetle, A. and Wang, X. (2015) Overexpression of patatin-related phospholipase AIII δ altered plant growth and increased seed oil content in camelina. *Plant Biotechnol. J.* **13**, 766–778.
- Lin, Y., Chen, G., Mietkiewska, E., Song, Z., Mark, K., Stacy, P.C., Dyer, J., Smith, M., McKeon, T. and Weselake, R.J. (2019) Castor patatin-like phospholipase A III β facilitates removal of hydroxy fatty acids from phosphatidylcholine in transgenic *Arabidopsis* seeds. *Plant Mol. Biol.* **101**, 521–536.
- van de Loo, F.J., Broun, P., Turner, S. and Somerville, C. (1995) An oleate 12-hydroxylase from *Ricinus communis* L. is a fatty acyl desaturase homolog. *Proc. Natl Acad. Sci. USA*, **92**, 6743–6747.
- Lu, C., Fulda, M., Wallis, J.G. and Browse, J. (2006) A high-throughput screen for genes from castor that boost hydroxy fatty acid accumulation in seed oils of transgenic *Arabidopsis*. *Plant J.* **45**, 847–856.
- Lu, C. and Kang, J. (2008) Generation of transgenic plants of a potential oil-seed crop *Camelina sativa* by *Agrobacterium*-mediated transformation. *Plant Cell Rep.* **27**, 273–278.
- Luddy, F.E., Barford, R.A., Herb, S.F., Magidman, P. and Riemenschneider, R.W. (1964) Pancreatic lipase hydrolysis of triglycerides by a semimicro technique. *J. Am. Oil Chem. Soc.* **41**, 693–696.
- Lunn, D., Wallis, J.G. and Browse, J. (2019) Tri-hydroxy-triacylglycerol is efficiently produced by position-specific castor acyltransferases. *Plant Physiol.* **179**, 1050–1063.
- McKeon, T.A. (2016) Castor (*Ricinus communis* L.). In *Industrial Oil Crops*. (McKeon, T.A., Hayes, D.G., Hildebrand, D.F. and Weselake, R.J., eds). New York/Urbana: Elsevier/AOCS Press, pp. 75–112.
- McKeon, T.A. and He, X. (2015) Castor diacylglycerol acyltransferase type 1 (DGAT1) displays greater activity with diricinolein than *Arabidopsis* DGAT1. *Biocatal. Agric. Biotechnol.* **1**, 276–278.
- Merkel, O., Fido, M., Mayr, J.A., Prüger, H., Raab, F., Zandonella, G., Kohlwein, S.D. and Paltauf, F. (1999) Characterization and function in vivo of two novel phospholipases B/lysophospholipases from *Saccharomyces cerevisiae*. *J. Biol. Chem.* **274**, 28121–28127.
- Mietkiewska, E., Miles, R., Wickramaratna, A., Sahibollah, A.F., Greer, M.S., Chen, G. and Weselake, R.J. (2014) Combined transgenic expression of *Punica granatum* conjugase (FADX) and FAD2 desaturase in high linoleic acid *Arabidopsis thaliana* mutant leads to increased accumulation of punicic acid. *Planta*, **240**, 575–583.
- Millar, A.A., Smith, M.A. and Kunst, L. (2000) All fatty acids are not equal: Discrimination in plant membrane lipids. *Trends Plant Sci.* **5**, 95–101.
- Moon, H., Smith, M.A. and Kunst, L. (2001) A condensing enzyme from the seeds of *Lesquerella fendleri* that specifically elongates hydroxy fatty acids. *Plant Physiol.* **127**, 1635–1643.
- Mouchlis, V.D., Bucher, D., Mccammon, J.A. and Dennis, E.A. (2014) Membranes serve as allosteric activators of phospholipase A₂, enabling it to extract, bind, and hydrolyze phospholipid substrates. *Proc. Natl Acad. Sci. USA*, **112**(6), E516–E525.
- Mubofu, E.B. (2016) Castor oil as a potential renewable resource for the production of functional materials. *Sustain. Chem. Process.* **4**, 1–12.
- Munnik, T. and Testerink, C. (2009) Plant phospholipid signaling: “in a nutshell”. *J. Lipid Res.* **50**, S260–S265.
- Noiriel, A., Benveniste, P., Banas, A., Stymne, S. and Bouvier-Navé, P. (2004) Expression in yeast of a novel phospholipase A1 cDNA from *Arabidopsis thaliana*. *Eur. J. Biochem./FEBS*, **271**, 3752–3764.
- Ogunniyi, D.S. (2006) Castor oil: a vital industrial raw material. *Biores. Technol.* **97**, 1086–1091.
- Ohta, S., Mita, S. and Hattori, T. (1990) Construction and expression in tobacco of a β -glucuronidase (*GUS*) reporter gene containing an intron within the coding sequence. *Plant Cell Physiol.* **31**, 805–813.
- Rauwerdink, A. and Kazlauskas, R.J. (2015) How the same core catalytic machinery catalyzes 17 different reactions: the serine-histidine-aspartate catalytic triad of α/β -hydrolase fold enzymes. *ACS Catal.* **5**, 6153–6176.
- Rietz, S., Dermendjiev, G., Oppermann, E., Tafesse, F.G., Effendi, Y., Holk, A., Parker, J.E., Teige, M. and Scherer, G.F. (2010) Roles of *Arabidopsis* patatin-related phospholipases in root development are related to auxin responses and phosphate deficiency. *Mol. Plant*, **3**, 524–538.
- Shockey, J., Lager, I., Stymne, S., Kotapati, H.K., Sheffield, J., Mason, C. and Bates, P.D. (2019) Specialized lysophosphatidic acid acyltransferases contribute to unusual fatty acid accumulation in exotic *Euphorbiaceae* seed oils. *Planta*, **249**, 1285–1299.
- Singer, S.D., Chen, G., Mietkiewska, E., Tomasi, P., Jayawardhane, K., Dyer, J.M. and Weselake, R.J. (2016) *Arabidopsis* GPAT9 contributes to synthesis of intracellular glycerolipids but not surface lipids. *J. Exp. Bot.* **67**, 4627–4638.
- Singer, S.D., Hily, J. and Liu, Z. (2010) A 1-kb bacteriophage lambda fragment functions as an insulator to effectively block enhancer-promoter interactions in *Arabidopsis thaliana*. *Plant Mol. Biol. Rep.* **28**, 69–76.
- Smith, M.A., Moon, H., Chowrira, G. and Kunst, L. (2003) Heterologous expression of a fatty acid hydroxylase gene in developing seeds of *Arabidopsis thaliana*. *Planta*, **217**, 507–516.
- Tian, B., Lu, T., Xu, Y., Wang, R. and Chen, G. (2019) Identification of genes associated with ricinoleic acid accumulation in *Hiptage benghalensis* via transcriptome analysis. *Biotechnol. Biofuels*, **12**, 1–16.
- Trifinopoulos, J., Nguyen, L.T., von Haeseler, A. and Minh, B.Q. (2016) W-IQ-TREE: a fast online phylogenetic tool for maximum likelihood analysis. *Nucleic Acids Res.* **44**, W232–W235.
- Troncoso-Ponce, M.A., Kilaru, A., Cao, X., Durrett, T.P., Fan, J., Jensen, J.K., Thrower, N.A., Pauly, M., Wilkerson, C. and Ohlrogge, J.B. (2011) Comparative deep transcriptional profiling of four developing oilseeds. *Plant J.* **68**, 1014–1027.
- Wang, X. (2001) Plant phospholipase. *Annu. Rev. Plant Physiol. Plant Mol. Biol.* **52**, 211–231.
- Xu, Y., Caldo, K.M.P., Jayawardhane, K., Ozga, J.A., Weselake, R.J. and Chen, G. (2019) A transferase interactome that may facilitate channeling of polyunsaturated fatty acid moieties from phosphatidylcholine to triacylglycerol. *J. Biol. Chem.* **294**, 14838–14844.